Journal of Chromatography B, 870 (2008) 178–185

Contents lists available at ScienceDirect

Journal of Chromatography B

journal homepage: www.elsevier.com/locate/chromb

A metabonomic characterization of CCl_4-induced acute liver failure using partial least square regression based on the GC/MS metabolic profiles of plasma in mice

Xin Huang[a], Li Shao[a], Yifei Gong[a], Yong Mao[a], Changxiao Liu[b], Haibin Qu[a,*], Yiyu Cheng[a,*]

[a] Pharmaceutical Informatics Institute, College of Pharmaceutical Sciences, Zhejiang University, Hangzhou 310058, China
[b] Tianjin Key Laboratory of Pharmacokinetics and Pharmacodynamics, Tianjin Institute of Pharmaceutical Research, Tianjin 300193, China

ARTICLE INFO

Article history:
Received 29 January 2008
Accepted 5 May 2008
Available online 6 June 2008

Keywords:
Metabonomics
PLS-RA
GC/MS
Carbon tetrachloride
Reactive oxygen species
Acute liver failure

ABSTRACT

This work characterized the metabolism disorders of acute liver failure (ALF) induced by carbon tetrachloride (CCl_4) in a mouse model with different dosage of intoxication (100, 500 and 1000 mg/kg). Metabolic profiles of mice plasma were detected by gas chromatography/mass spectrometry (GC/MS) after chemical derivatization. Here an effective information-extracting approach was implemented on the basis of partial least square regression analysis (PLS-RA). PLS modeling was achieved with two kinds of *Y*-vectors for the acquired metabonomics data and eight metabolites with different changing behaviors were selected. ALF of mice induced by CCl_4 was characterized by the elevation of glutamate, citrate, serine and threonine, as well as the decrease of α-glycerophosphate, docosahexaenoic acid, palmitic acid and oleic acid in plasma. The difference in the concentrations of serine, threonine, palmitic acid and oleic acid remained insignificant between the control and 100 mg/kg groups, while significant distinction appeared when comparing the control and two higher dosed groups. The underlying regulation of CCl_4-perturbed metabolic pathways was discussed according to the selected metabolites. The present study demonstrated a great potential of PLS-RA in exploiting a comprehensive metabolic effects of CCl_4 intoxication and its efficient capability to reveal the hepatotoxic mechanism of ALF induced by reactive oxygen species (ROS).

1. Introduction

Acute liver failure (ALF) is a rare condition consisting of rapid-onset severe liver injury accompanied by coagulopathy and encephalopathy, with a mortality rate of approximately 90% in patients [1,2]. Approximately 2000 cases per year occur in the US resulting in liver transplantation or death in more than 35% of these cases, frequently due to multiorgan failure (MOF). Nevertheless, etiology of ALF is mysterious in approximately 20% of adult patients in the US [3]. In addition, clinic trials of ALF are still difficult to perform since the scantiness of available clinic samples with both poor diagnosis and prognosis [2].

So far, specific metabolic disorders and metabolic syndromes of ALF have been investigated in literature [4–6]. Integrated approaches delineating the comprehensive metabolic perturbation of ALF are still necessary on the basis of clinic diagnostic and therapeutic researches. Metabonomics, defined as "the quantitative measurement of the dynamic multiparametric responses of a living system to pathophysiological stimuli or genetic modification" [7], aims to this destination and is gaining increasing appreciation in recent years [7–12]. Until now, metabonomic approach has proved profitable in providing valuable site- and pathway-related information of metabolic profiles from a variety of biofluids such as urine, plasma and cerebrospinal fluid, etc. [13–15]. Since metabonomics depends on the ability to describe the changes of low molecular-weight metabolites in various biofluids, analytical methods such as NMR and MS based platforms, should produce comprehensive profiles of metabolites from the biological samples. Among these analytical techniques, the GC/MS method has been proved both robust [16,17] and effective [11,12], and gained increased implementation recently in performing the global metabolic profiles.

As a new member in system biology, metabonomics has the obligation to demonstrate a temporal but comprehensive interpretation of metabolic changes to various interventions [18]. In general,

Abbreviations: ALF, acute liver failure; GC/MS, gas chromatography/mass spectrometry; ROS, reactive oxygen species; MOF, multiorgan failure; PCA, principle component analysis; PLS-RA, partial least square regression analysis; LV, latent variable; TMCS, trimethylchlorosilane; MSTFA, *N*-methyl-*N*-trimethylsilyltrifluoroacetamide; RSD, relative standard deviation; TCA, tricarboxylic acid; AA, amino acid or arachidonic acid; β-HB, β-hydroxybutyrate; DHB, 2,4-dihydroxybutyrate; AMA, aminomalonic acid; AGP, α-glycerophosphate; POA, palmitoleic acid; PA, palmitic acid; LOA, linoleic acid; OA, oleic acid; IOA, isooleic acid; SA, steric acid; DHA, docosahexaenoic acid; PAG, palmitic acid glyceride; SAG, steric acid glyceride; RP, ribose phosphate; PUSFA, polyunsatured fatty acids; VLDL, very low density lipoprotein, amino acids in this work are abbreviated using the standard three-letter convention.

* Corresponding authors. Tel.: +86 571 87951138; fax: +86 571 87951138.
E-mail addresses: quhb@zju.edu.cn (H. Qu), chengyy@zju.edu.cn (Y. Cheng).

1570-0232/$ – see front matter © 2008 Elsevier B.V. All rights reserved.
doi:10.1016/j.jchromb.2008.05.049

multivariate statistical methods such as principal component analysis (PCA) [11–14] and partial least square (PLS) method [19] are popular in handling the acquired metabonomics data. PLS method can afford not only good classifications of observations, but also extract information-rich latent structures by regression during the modeling [20]. Regression analysis (RA) with PLS hence becomes a good choice and the regression coefficient of each variable is capable to illustrate both the correlation and changing direction of corresponding metabolite. So PLS-RA provides a rapid visualization of the perturbed metabolites and leads to a comprehension of regulation for the relevant pathways.

Reactive oxygen species (ROS) are one causative factor in the etiology of multiorgan degenerative diseases, including ALF and other hepatopathies [21]. The oxygen free radicals and oxidative stress enhanced by ROS are considered as a critical incentive of massive hepatocyte necrosis accompanied with fulminant impairments of the whole living system [22]. Threaten of ROS-induced ALF can be caused by a variety of factors, including environmental contaminants and exposure to some industrial chemicals (acetone, trichloromethane and carbon tetrachloride, etc.) [23,24]. Moreover, it is reported that the hepatotoxic mechanism of some drug-induced ALF, such as acetaminophen, is related to ROS [25]. In this study, CCl_4-induced acute liver injure in mice was introduced to investigate ROS-induced ALF using metabonomics methodology. Through the detection of metabolic difference of mice plasma analyzed by GC/MS, we aimed (i) to demonstrate the great potential of the proposed PLS-RA based data-processing method in metabonomics; (ii) to investigate the overall metabolic disorders and relevant disturbed pathways of ALF induced by ROS and (iii) to provide a complementary approach consisted of several metabolites in monitoring ALF, whether the liver damage can be auto-regulated or irreversible fulminate.

2. Experimental

2.1. Chemical and reagents

N-methyl-*N*-trimethylsilyltrifluoroacetamide (MSTFA), trimethylchlorosilane (TMCS), docosane, methylhydroxylamine hydrochloride, and pyridine were of analytical grade and purchased from Fluka (Buchs, Switzerland). Carbon tetrachloride, natural amino acids, oxalate, malic acid, citric acid, D-ribose, galactose, glucose, palmitic acid, and steric acid were of analytical grade from China National Pharmaceutical Group Co. (Shanghai, China). Unsaturated fatty acids (oleic acid, linoleic acid, arachidonic acid, and docosahexaenoic acid) were of GC grade (purity >98%) and purchased from Sigma Co. (St. Louis, MO, USA).

2.2. Animal study and sample collection

Twenty-four male ICR mice (20 ± 2 g) were purchased from the Animal Center of Zhejiang Province (Hangzhou, China). These mice were acclimated for one week at a temperature around 20 °C and a relative humidity around 40%, with a 12 h light/12 h dark cycle. Food and tap water were provided ad libitum. After a fast of 12 h before treatment, they were divided into four groups randomly ($n = 6$), including the control group (bean oil only), low dosed group (CCl_4, 100 mg/kg, i.p., dissolved in bean oil), middle dosed group (500 mg/kg) and high dosed group (1000 mg/kg). Animals were sacrificed 48 h post-administration and plasma was quickly collected. A left lobe of the liver tissue was collected and fixed in 10% formalin for 12 h, embedded in paraffin wax and stained with hematoxylin–eosin (H–E). Stained samples were examined using an inversed optical microscopy (Leica Microsystems wetzlar GmbH, Germany) and photomicrographs of liver tissue were achieved through an equipped CCD camera.

2.3. Samples preprocessing and GC/MS analysis

In this study, processing of the plasma samples followed a protocol described in ref. [26] but with minor modifications. Briefly, 250 μL of acetonitrile was added into 100 μL of plasma for protein-precipitation (kept on ice for 15 min), then followed by centrifugation (10 000 g, 10 min, 4 °C). 150 μL of the supernatant was transferred to a GC vial and evaporated under a stream of nitrogen gas to dryness. Methoxymation was carried out at 70 °C for 1 h after methylhydroxylamine hydrochloride (50 μL, 15 mg/mL in pyridine) was added. MSTFA (50 μL, with 1% TMCS as the catalyst) was added, and the trimethylsilylation was performed at 70 °C for 1 h. After adding 150 μL *n*-heptane (containing 0.10 mg/mL of docosane, reference compound) and vortex mixing, the derivatized sample was transferred to a GC microvial after filtration.

The samples were analyzed on an Agilent 6890 gas chromatograph equipped with a 5973 mass selective detector and a 7683 injector (Agilent Technologies, Palo Alto, CA). A ZB-5MS fused-silica capillary column (0.25 mm × 30 m × 0.25 μm, Phenomenex, USA) was used for the separation with a helium carrier gas flow of 1.0 mL/min. 2.0 μL of derivatized samples was injected into the GC/MS instrument. To acquire a well separation, the GC oven was initially held at 85 °C for 5 min, and increased to 300 °C at a rate of 10 °C/min, where it was held for 5 min. Splitless mode was used and the electron energy was set at 70 ev. MS detection was implemented with electron ionization mode and full scan mode (m/z 60–600).

2.4. Identification of the endogenous metabolites

All collected plasma samples were analyzed and low molecular-weight metabolites were represented as the chromatographic peaks in the GC total ion current (TIC) chromatograms. EI-MS spectra of these peaks were interpreted using AMDIS (version 2.1, DTRA/NIST, USA) software and a majority of them can be well identified based on the NIST library 2002. Furthermore, identification of metabolites was performed using the commercial available standards by comparing their MS spectra and retention time, including twenty kinds of natural amino acids, the major organic acids, saccharides, fatty acids in biofluids, and cholesterol.

2.5. Data deconvolution and pattern recognition

Useful information was involved in these GC/MS data such as the retention characteristics, intensities (peak areas) and the MS spectra of the endogenous metabolites. In order to handle the complex metabonomics data, a matrix of peaks present in the collected samples must be generated. For this purpose, data denoising and peak detection were performed firstly based on the TIC chromatogram, using Agilent Enhanced ChemStation software (Agilent Technologies). The commensal peaks were aligned to generate a two-dimensional data table, in which rows and columns represent the samples and the relative peak areas of commensal metabolites, respectively. The resulting data table (CSV file) was imported into the SIMCA-P (version 11, Umetrics AB, Sweden) software for the multivariate analysis. Principal component analysis was applied with auto-scaling pretreated before. Partial least square method was performed with two different *Y*-vectors. Some metabolites were highlighted through their regression coefficients in PLS regression. Finally, significance of the between-group difference for these metabolites was examined by the students *T*-test using customer Matlab (version 6.5, Math Works, USA) scripts.

3. Results

3.1. Histopathological assessment for CCl_4-induced liver injure

The liver sections stained with H–E were examined for the histopathological assessment of CCl_4-induced liver injury. Extensive liver damage areas were observed in most CCl_4 challenged samples. As shown in Fig. 1, samples from the 100 mg/kg dosed group illustrate mild degrees of liver damage. But in the 500 and 1000 mg/kg dosed samples, hepatocytes surrounding the central vein and perivenular regions exhibited serious coagulative-type necrosis. Many hepatocytes in CCl_4 treated groups appeared pyknotic nuclei in the necrotic area. Severe liver inflammation and congestion were noted in the 500 and 1000 mg/kg dosed groups, compared with the normal liver morphologies observed in the control group.

3.2. GC/MS metabolic profiling of plasma

A typical GC/MS TIC chromatogram of mice plasma is displayed in Fig. 2, and images of the low-intensity regions are zoomed in, respectively. At the first glance, the number of features does not seem particularly high. Magnifying the low-intensity regions of the TIC trace gives an impression of a large number of individual peaks observed using this technique. As shown in Fig. 2, most of the low molecular-weight endogenous metabolites, such as amino acids, organic acids, carbohydrates, fatty acids and steroids, were eluted sequentially from the GC capillary column. These compounds are involved in many biochemical processes in bio-systems, especially the amino acid metabolism, energy metabolism and lipid metabolism.

The applied GC/MS method was validated prior to the analysis of the experimental samples, including the precision of injection, the within-day stability and the repeatability of sample preparation. Precision of injection was carried out by the continuous detection of six injections of the same sample, and the relative standard deviations (RSDs) of peak intensities for each commensal metabolite were calculated. RSDs of the main peaks in plasma ranged from 2.16% to 9.85%. Within-day stability was investigated by a totally six injections in 24 h with an interval of 4 h from the same plasma sample after preparation. Then six parallel samples were prepared using the same preparation protocol. As a result, RSDs of the main peaks ranged from 1.24% to 15.09% for the within-day stability test, and ranged from 2.45% to 13.97% for the repeatability test, respectively.

In general, more than one hundred peaks were detected approximately with the intensity higher than 3-fold of the signal-to-noise ratio from each GC/MS run. Then the detected peaks were aligned, mainly based on their retention similarity. Peaks of lactic acid, urea, phosphatic acid and glucose were overloaded in the GC/MS profiles with the current concentration, and therefore excluded from the next processing procedures. Meanwhile, peaks identified as the solvents and reagents, as well as several unidentified compounds, were also removed from the GC/MS data. At last, 37 peaks were achieved as the commensal endogenous metabolites, which were used to construct a 37-dimensional vector to characterize the metabolic pattern (profile) of mice plasma.

3.3. Principal component analysis and partial least square regression analysis

Principal component analysis is performed firstly for the acquired metabonomics data table. The modeling diagnostic of PCA in this study is summarized in Table 1. The 1st and 2nd component explained 36.4% and 13.5% of the systematic variation, respectively. The PCA score plot is displayed in Fig. 3. The control group tended to cluster to the left part, while locations of dosed groups generally moved right away from the controls with an increased CCl_4 dosage.

Partial least square is a supervised statistical method and additional knowledge (*Y*-variables) must be included to "supervise" the independent data (*X*-variables). In this study, regression analysis

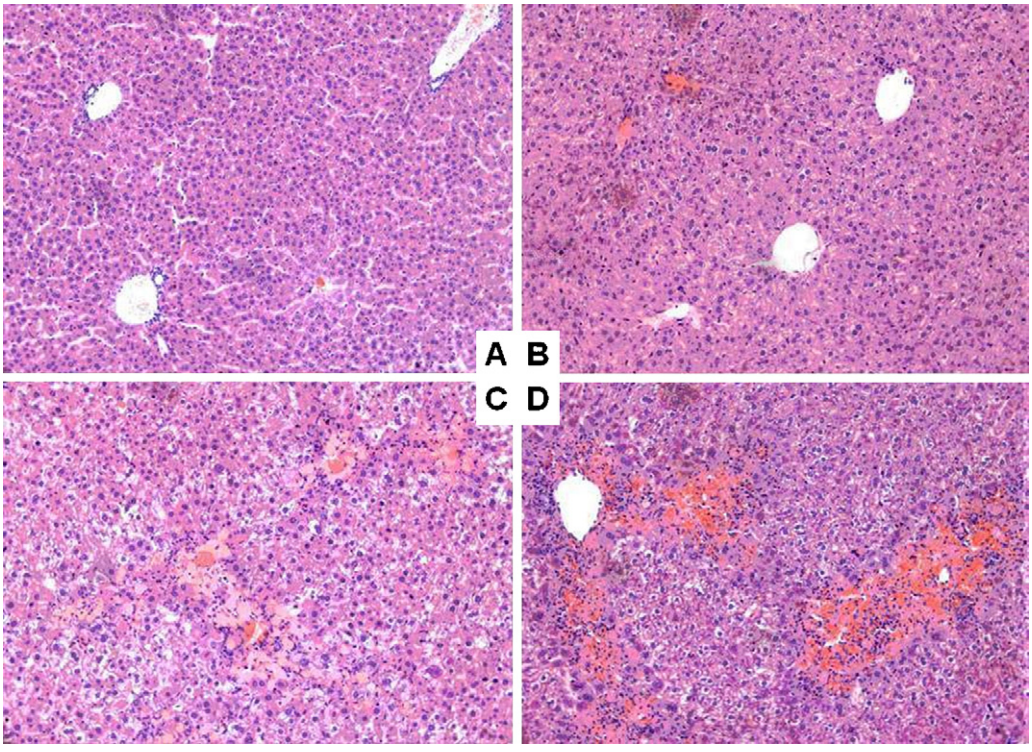

Fig. 1. Photomicrographs of the liver tissues in mice with different CCl_4 intoxication: A, control; B, 100 mg/kg; C, 500 mg/kg; D, 1000 mg/kg.

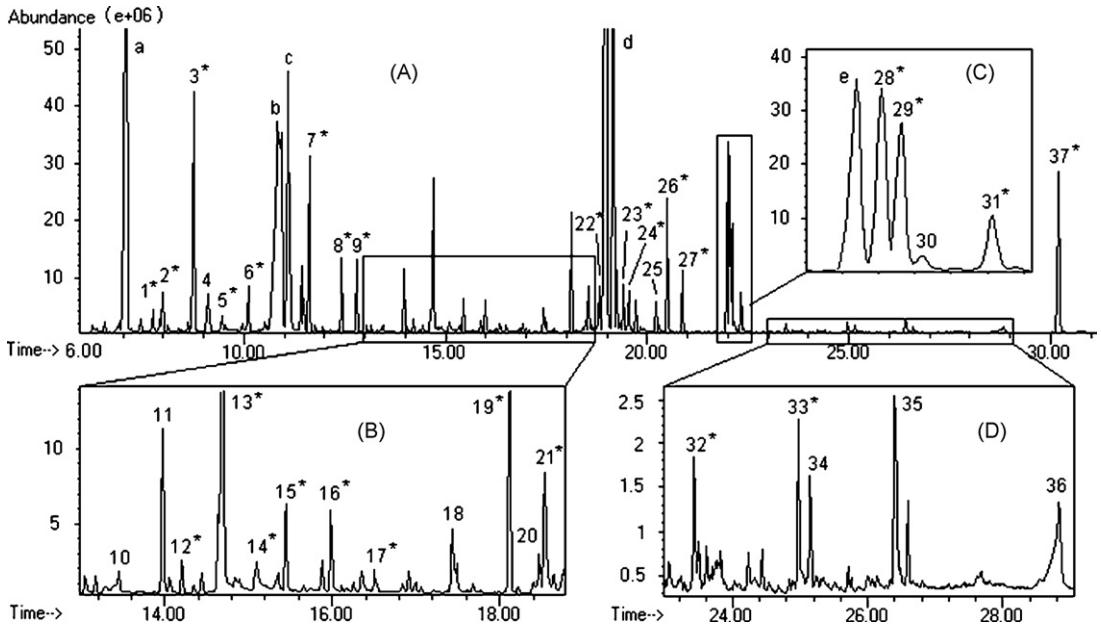

Fig. 2. Metabolic profile of mice plasma is illustrated as the total ion current (TIC) chromatogram in GC/MS analysis. The whole profile is shown in subfigure A and specific areas of it is magnified in subfigures B, C, and D. Overloaded metabolites: a, lactic acid; b, urea; c, phosphatic acid; d, glucose. Peak e is docosane (reference compound). Selected commensal metabolites: 1, alanine (Ala); 2, aspartate (Asp); 3, oxalate; 4, β-hydroxybutyrate (β-HB); 5, isoleucine (Ile); 6, valine (Val); 7, glycine (Gly); 8, serine (Ser); 9, threonine (Thr); 10, 2,4-dihydroxybutyrate (DHB); 11, aminomalonic acid (AMA); 12, malate; 13, proline (Pro) 14, glutamate (Glu); 15, glutamine (Gln); 16, phenylalanine (Phe); 17, D-ribose; 18, α-glycerophosphate (AGP); 19, citrate; 20, ornithine (Orn); 21, fructose; 22, galactose; 23, lysine (Lys); 24, glucitol; 25, palmitoleic acid (POA); 26, palmitic acid (PA); 27, myoinositol; 28, linoleic acid (LOA); 29, oleic acid (OA); 30, isooleic acid (IOA); 31, steric acid (SA); 32, arachidonic acid (AA); 33, docosahexaenoic acid (DHA); 34, palmitic acid glyceride (PAG); 35, steric acid glyceride (SAG); 36, ribose phosphate (RP); 37, cholesterol. An asterisk behind the peak number indicates this metabolite has been further identified by the commercial standards.

was performed using PLS, with the *Y*-variables containing for two kinds of discrete vectors. There are (i) four-level PLS-RA: the *Y*-vector of samples from the control, 100, 500 and 1000 mg/kg groups were marked as 0, 1, 2, and 3, respectively; and (ii) two-level PLS-RA: *Y*-vector from the control and 100 mg/kg groups were marked as 0, and the other two groups were marked as 1. The PLS diagnostic is tabulated in Table 1 after modeling. Here R^2X and R^2Y are the fractions of *X*-variation and *Y*-variation modeled for specific component, respectively. Q^2Y is the estimate of how well the model predicts the *Y*-variables through a default 7-fold cross-validation. The cumulative values of R^2Y and Q^2Y of the selected components close to one indicate a perfect fitting. So the diagnostic results indicated both these PLS-RA models demonstrated good performances based on the acquired metabonomics data. The PLS score plots (Fig. 4) are shown for the four-level and two-level regression, respectively.

Table 1
Modeling diagnostic of the metabolic profiling data

Model	Components		Modeling diagnostic		
			R^2X	R^2Y	Q^2
PCA	4	c	0.691	–	–
		f	0.364	–	–
Four-level PLS	2	c	0.453	0.939	0.841
		f	0.362	0.857	0.828
Two-level PLS	2	c	0.472	0.936	0.878
		f	0.361	0.859	0.827

Note. Component is the number of the extracted latent variables; R^2X is the fraction of *X*-variation; R^2Y is the fraction of *Y*-variation; Q^2 is the cumulated cross-validation for R^2Y. R^2X, R^2Y and Q^2 are all ranged from 0 to 1. R^2X indicates how well the *X*-variables fit the *Y* data, R^2Y indicates how well the *X*-variables predict the *Y* data, and Q^2 indicates the goodness of fit from the cross-validation. The label "c" indicates the cumulated contribution of the selected components for the modeling diagnostic, while the label "f" specifies the corresponding contribution for the first component.

3.4. Highlighted metabolites by regression analysis

In regression analysis, a measurement named regression coefficients basically express how strong the dependent *Y*-variable is correlated to the extracted components (also called latent variables, LVs) from the systematic information of *X*-variables. As tabulated in Table 1, the first component of four-level PLS-RA explains a variation (R^2X) of 0.362 for the *X*-variables, and a variation (R^2Y) of 0.857 for the *Y*-variable. In two-level PLS-RA, the diagnostic for the first component was $R^2X = 0.361$, and $R^2Y = 0.859$. The first components of these two models were both capable to represent the major distinctions of systematic information, and hence the correlation coefficient for each metabolite was calculated between the first components and the *Y*-variables in the two PLS-RA models, respectively.

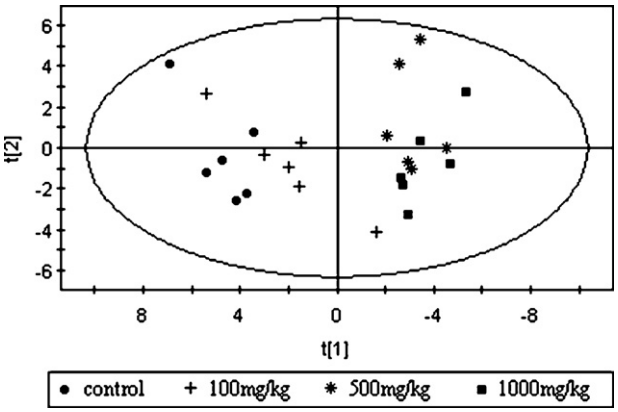

Fig. 3. PCA score plots of the control group and the CCl_4 treated groups by GC/MS analysis, with auto-scaling applied before. Samples with different treatment were illustrated at the bottom of the figure.

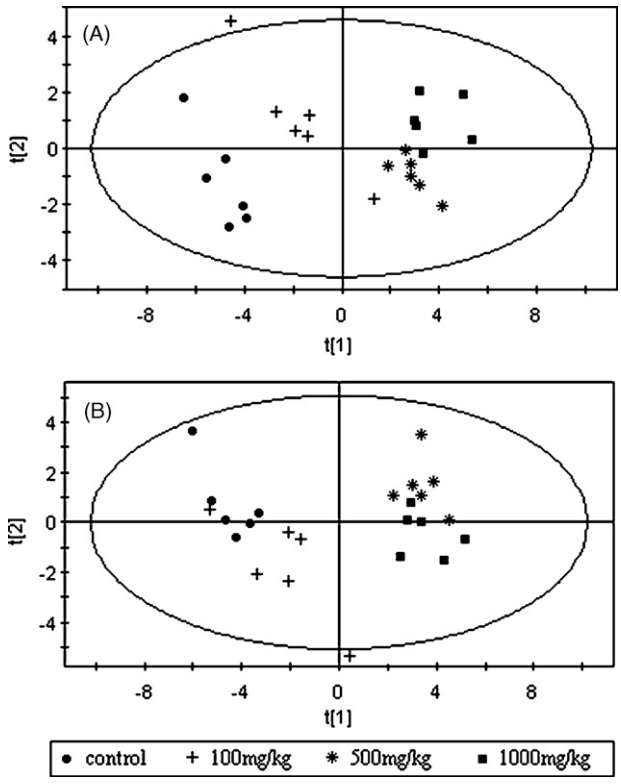

Fig. 4. PLS score plots of the control group and the CCl_4 treated groups by GC/MS analysis. PLS-RA was performed with both four-level (A) and two-level (B) regression. Samples with different treatment were illustrated as the bottom of the figure.

In PLS-RA, a rapid visualization can be achieved through the "coefficient plot" (Fig. 5). Here a confidence interval for each coefficient was calculated according to a significant level (α is 0.05 in this study) [20]. A large absolute value of the regression coefficient indicates a high correlation between the *X*- and *Y*-variables, either positive or negative. Moreover, this coefficient can be considered significant (above the noise) in regression if its confidence interval does not cross zero. In order to demonstrate the potential of these two regression strategies, four metabolites were firstly selected from coefficient plot (Fig. 5A) of the four-level PLS-RA, two of which (citrate and glutamate) had the maximal coefficient values, while the other two (α-glycerophosphate (AGP) and docosahexaenoic acid (DHA)) had the minimal values. Correspondingly, another four metabolites (serine, threonine, palmitic acid and oleic acid) were selected from coefficient plot (Fig. 5B) of the two-level PLS-RA.

The selected metabolite was illustrated as mean concentration and standard variation (S.D.) in each experimental group, respectively. As shown in Fig. 6A, citrate and glutamate were selected with the largest two coefficient values from the four-level PLS-RA. Concentrations of these two metabolites increased gradually from the control to the 1000 mg/kg dosed groups. On the contrary, concentrations of AGP and DHA decreased gradually while increasing the CCl_4 dosage (Fig. 6B). For the highlighted metabolites in two-level PLS-RA, concentrations of serine and threonine were found insignificantly different between the control and 100 mg/kg dosed groups. However, these two metabolites, illustrated dramatically augment of their concentrations in 500 and 1000 mg/kg dosed groups, compared with the former two groups (Fig. 6C). Concentrations of palmitic acid and oleic acid also reflected similar tendencies. Nearly no differences were detected of their concentrations between the control and 100 mg/kg dosed groups, while significant reduction appeared when comparing the control and two higher dosed groups (Fig. 6D).

4. Discussion

4.1. Pattern recognition of the metabonomics data

PCA is an unsupervised pattern recognition method that attempts to explain as much variation as possible in as few components as possible. It is illustrated that the bio-effect of CCl_4 is generally dose-dependent from the PCA score plot (Fig. 3). Samples of the 100 mg/kg group locate between the control and two higher dosed groups. It was demonstrated that although the metabolic patterns of them have been disturbed, the patterns were still not deviated as seriously as the higher dosed samples. There was somewhat overlap between the 500 and 1000 mg/kg dosed groups, indicating that the metabolic patterns might not be further deteriorated by this double of the CCl_4 dosage.

In the PLS modeling, the *Y*-variables in regression can be both quantitative and qualitative [18]. For the qualitative analysis (so-called PLS discriminant analysis), a "dummy" matrix should be yielded as the *Y*-variable for the discrimination of a two-class dataset [19]. Other applications have adopted the dosage of administration as the *Y*-variable in regression [20]. In this study, it was demonstrated that the disturbed metabolic patterns and the intoxicant dosage of CCl_4 were not directly quantitative-correlated in the PCA modeling. Thus a discrete vector was employed as the *Y*-variable in the four-level PLS-RA. Furthermore, samples at a dosage of 100 mg/kg indicated an intermediate metabolic pattern between the control and seriously disturbed groups. The physiological status of this group can be considered relative "healthy", compared with the 500 and 1000 mg/kg dosed groups. Therefore, the two-level PLS-RA was applied, so as to investigate the distinctions of between the slightly and heavily disturbed metabolic profiles after CCl_4 treatment.

The coefficient plots of PLS-RA are displayed in Fig. 4. Here both the capacity of correlation and the direction of regulation (up- and down-regulated) for each metabolite can be directly comprehended in this deploying. At last, distinct changing behaviors of the selected metabolites were illustrated between the control and CCl_4 treated groups. The biochemical mechanism for the regulations of the metabolic network after CCl_4 challenge might be revealed from the highlighted eight metabolites.

4.2. Carbon tetrachloride-induced acute hepatotoxicity

CCl_4 is widely employed as an experimental toxin and the free radicals (ROS) accompanied by oxidative stress were considered as the main principle of CCl_4-induced acute liver injures [27]. Changing behaviors for the concentrations of the selected marker metabolites were illustrated in Fig. 6. Firstly, glutamate and citrate are two important energy-supply substances in plasma for the mitochondrial tricarboxylic acid (TCA) cycle. Under oxidative stress, TCA cycle is slowed down in cellular regulation to reduce the natural production of ROS [28]. So we infer that the augment of glutamate and citrate is due to the dysfunction of mitochondria and the block of natural energy production by CCl_4 intoxication. Secondly, the peroxidation of polyunsatured fatty acids (PUSFA), especially the arachidonic acid and DHA, is a feature cell injure intermediated by ROS [29]. AGP is the structural molecular to constitute phospholipids. So the diminish of AGP and DHA in plasma could be explained as a cascade of metabolic compensatory regulation for the phospholipids re-synthesis to combat the degradation of normal structure components. Thirdly, it has already been

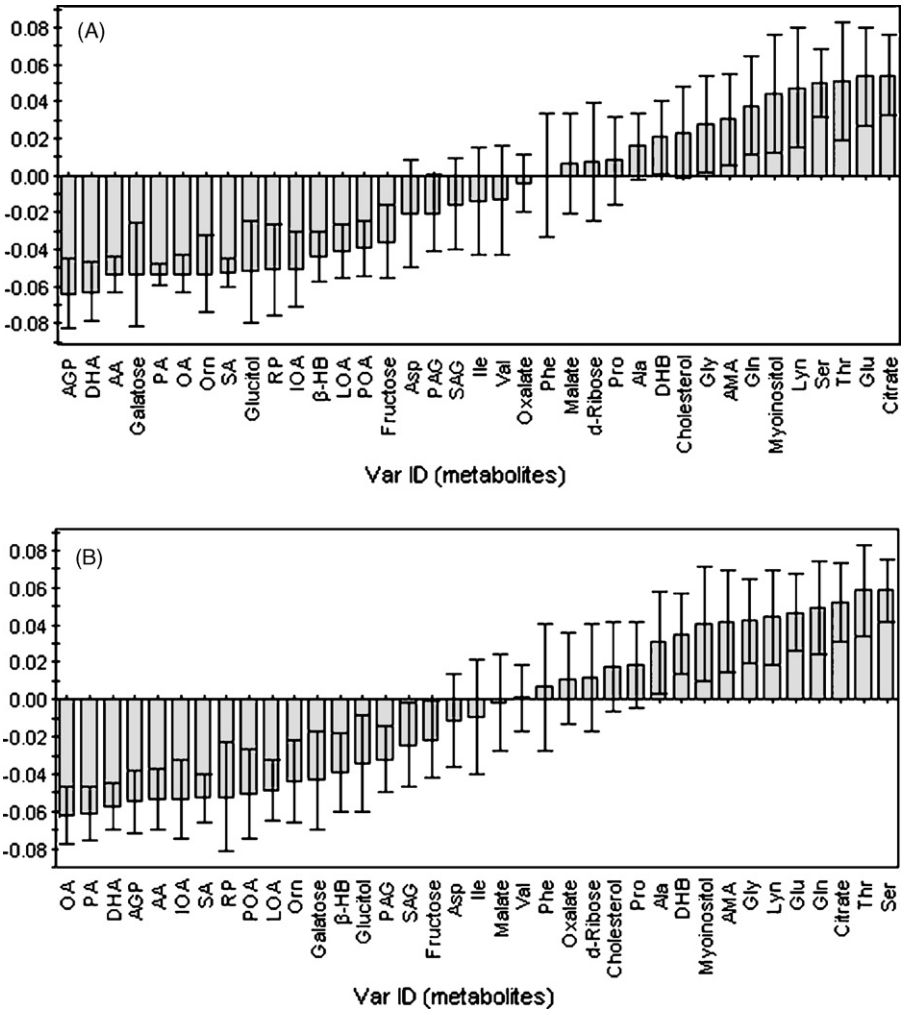

Fig. 5. PLS-RA coefficient plots of the metabolites according to both the four-level (A) and two-level (B) regression. The confidence interval ($\alpha = 0.05$) in the PLS-RA model for each variable (metabolite) was marked as a bi-lateral bar on each column. A metabolite with a coefficient value above zero indicated that it is up-regulated after the CCl_4 challenge compared with the control group, and vice versa. Metabolites were aligned in ascending order of their coefficient values. Some metabolites were abbreviated as proposed in the legend of Fig. 2.

proposed that CCl_4 intoxication can decay amino acid (AA) uptake and proteins synthesis [22]. In addition, both gluconeogenesis and glycolysis are inhibited under oxidative stress [28]. Concentrations of most AA were found increased after the CCl_4 challenge in this study. Serine and threonine are two typical gluconeogenic AA to synthesize hepatic glucose, or entry into the TCA cycle through acetyl-CoA or succinyl-CoA by anaplerosis. So we infer that the increased serine and threonine in our study was mainly caused by the inhibition of gluconeogenesis and relevant AA uptake. Finally, concentrations of palmitic acid and oleic acid were found decreased. This phenomenon could be explained as the inhibition of lipoproteins synthesis by hepatic enzymes dysfunction, especially the synthesis of very low density lipoproteins (VLDL). Since VLDL is a critical hepatic protein required for the transport and secretion of lipids from liver to plasma [22].

4.3. Mechanism of ROS-induced AFL

Mechanisms of AFL caused by CCl_4 can be divided into two stages: firstly, free radicals initiate lipid peroxidation of PUSFA and depletion of cellular reductive agents; secondly, when the amount of ROS production exceeds the capacity of the endogenous cellular antioxidant system, the normal function of major organelles may be impaired, resulting in significant liver injury [27]. Considering the possibility that the group given more CCl_4 may be more severely injured at the same time-point postdose, it is supposed that the biochemical information implicated in the selected metabolites may be capable to represent the perturbations of relevant pathways occurring in those two stages of liver injury.

According to the proposed biochemical paraphrase in this study, glutamate, citrate, AGP and DHA are directly related to the disturbed pathways and metabolic regulation induced by ROS, so the severity of ALF can be well reflected by the concentrations of these metabolites. Serine and threonine relate to the inhibited gluconeogenesis and relevant AA uptake. Palmitic acid and oleic acid relate to the liver lipoprotein synthesis dysfunction. So these mechanisms can be somewhat considered as “indirect” perturbations. In this study, concentrations of glutamate, citrate, AGP and DHA generally followed a gradual increase or decrease from the control to the highest dosed groups. But concentrations of serine, threonine, palmitate and oleate had nearly not different between the control and 100 mg/kg dosed samples, while entirely different from the 500 and 1000 mg/kg dosed samples. Therefore, it was inferred that the physiological status of 100 mg/kg dosed mice might remain in the first stage, since the proposed “indirect” pathways were not

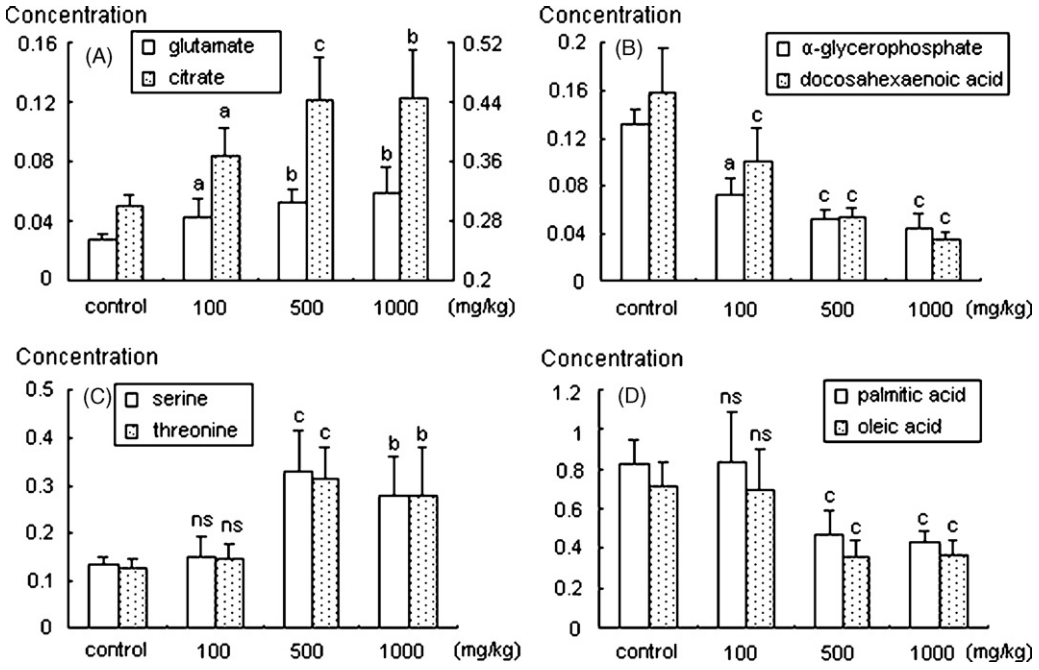

Fig. 6. Changing behaviors of the metabolites selected by their regression coefficients in PLS-RA. Glutamate and citrate (A) had the maximal values of coefficient in the four-level regression, while α-glycerophosphate and docosahexaenoic acid (B) had the minimal values. Serine and threonine (C), as well as palmitic acid and oleic acid (D) had the biggest and smallest coefficient values in the two-level regression, respectively. Metabolite was illustrated as the mean concentration in each group and standard derivation (S.D.) was marked on each column. Concentration of citrate uses the right (second) axes in subfigure A. Significant difference (ns, not significant; a, $p < 0.05$; b, $p < 0.01$; c, $p < 0.001$) between the CCl_4 treated groups and the control group was evaluated for each metabolite by the *T*-test.

under-regulated yet. And the liver injure might transit to the second stage if the CCl_4 intoxication was enhanced enough since prominent and all-around metabolic disorders were detected in the plasma with higher CCl_4 dosage.

5. Conclusion

ROS-induced acute liver damage is still a challenging field for the clinic and experimental hepato-toxicological studies of AFL. In this work, a PLS-RA based information-extracting method was provided to identify and characterize the CCl_4-induced metabolic disorders. The metabolic difference between the controls and the intoxicant samples with different CCl_4 dosage were examined by PLS-RA with two regression vectors on the acquired GC/MS metabolite profiling data. It was demonstrated that two stages of liver injure were initiated by CCl_4 intermediated free radicals. Severity of ALF could be reflected through the metabolites directly involved in the pathways of ROS-induced liver damage. However, metabolites involved in the indirect regulation might follow a dyadic manner. That is, normal physiological status was kept at a low level of intoxication while fatal and irreversible liver failure fulminated at a higher level. According to the investigations in this work, the significant elevation of gluconeogenic amino acids and depletion of free fatty acids in plasma might be adopted as the potential metabolic signals in monitoring ROS-induced ALF.

Acknowledgements

This work was financially supported by the Key Program of Zhejiang Province (No. 2005C13026), National Basic Research Programs of China (No. 2005CB523402), Postdoctoral Science Foundation of China (No. 20070410397), and Natural Science Foundation of China (No. 30772615).

References

[1] P. Caraceni, D.H. Van Thiel, Lancet 345 (1995) 163.
[2] J.G. O'Grady, G.J. Alexander, K.M. Hayllar, R. Williams, Gastroenterology 97 (1989) 439.
[3] G. Ostapowicz, R.J. Fontana, F.V. Schiodt, A. Larson, T.J. Davern, S.H. Han, T.M. McCashland, A.O. Hakil, J.E. Hay, L. Hynan, J.S. Crippin, A.T. Blei, G. Samuel, J. Reisch, W.M. Lee, Ann. Intern. Med. 137 (2002) 947.
[4] A.M. Larson, J. Polson, R.J. Fontana, T.J. Davern, E. Lalani, L.S. Hynan, J.S. Reisch, F.V. Schiødt, G. Ostapowicz, A.O. Shakil, W.M. Lee, Hepatology 42 (2005) 1364.
[5] C. Zwingmann, N. Chatauret, D. Leibfritz, R.F. Butterworth, Hepatology 37 (2003) 420.
[6] K. Arai, K. Lee, F. Berthiaume, R.G. Tompkins, M.L. Yarmush, Hepatology 34 (2001) 360.
[7] J.K. Nicholson, J.C. Lindon, E. Holmes, Xenobiotica 29 (1999) 1181.
[8] J.K. Nicholson, J. Connelly, J.C. Lindon, E. Holmes, Nat. Rev. Drug Discov. 1 (2002) 153.
[9] J.K. Nicholson, I.D. Wilson, Nat. Rev. Drug Discov. 2 (2003) 668.
[10] M. Rantalainen, O. Cloarec, O. Beckonert, I.D. Wilson, D. Jackson, R. Tonge, R. Rowlinson, S. Rayner, J. Nickson, R.W. Wilkinson, J.D. Mills, J. Trygg, J.K. Nicholson, E. Holmes, J. Proteome Res. 5 (2006) 2642.
[11] K. Yu, G. Sheng, J. Sheng, Y. Chen, W. Xu, X. Liu, H. Cao, H. Qu, Y. Cheng, L. Li, J. Proteome Res. 6 (2007) 2413.
[12] B. Feng, S. Wu, S. Lv, F. Liu, H. Chen, X. Yan, Y. Li, F. Dong, L. Wei, J. Proteome Res. 6 (2007) 2161.
[13] N.J. Waters, E. Holmes, A. Williams, C.J. Waterfield, R.D. Farrant, J.K. Nicholson, Chem. Res. Toxicol. 14 (2001) 1401.
[14] J. Yang, G. Xu, Y. Zheng, H. Kong, T. Pang, S. Lv, Q. Yang, J Chormatogr. B. 813 (2004) 59.
[15] M. Coen, Y.S. Hong, T.A. Clayton, C.M. Rohde, J.T. Pearce, M.D. Reily, D.G. Robertson, E. Holmes, J.C. Lindon, J.K. Nicholson, J. Proteome Res. 6 (2007) 2711.
[16] Y. Qiu, M. Su, Y. Liu, M. Chen, J. Gu, J. Zhang, W. Jia, Anal. Chim. Acta 583 (2007) 277.
[17] Q. Zhang, G. Wang, Y. Du, L. Zhu, A. J, J. Chromatogr. B 854 (2007) 20.
[18] J. Trygg, E. Holmes, T. Lundstedt, J. Proteome Res. 6 (2007) 469.
[19] S. Wagner, K. Scholz, M. Donegan, L. Burton, J. Wingate, W. Volkel, Anal. Chem. 78 (2006) 1296.
[20] H. Antti, T.M. Ebbels, H.C. Keun, M.E. Bollard, O. Beckonert, J.C. Lindon, J.K. Nicholson, E. Holmes, Chemometrics Intell. Lab. Syst. 73 (2004) 139.
[21] G. Poli, Br. Med. Bull. 49 (1993) 604.
[22] N. McIntyre, J.-P. Benhamou, J. Bircher, M. Rizzetto, J. Rodes, Oxford Textbook of Clinical Hepatology, Oxford University Press, Oxford, 1991.

[23] B. Nardo, P. Caraceni, L. Puviani, A.M. Pertosa, M. Domenicali, M. Pariali, G. Angiolini, P. Chieco, F. Trevisani, M. Bernardi, A. Cavallari, J. Surg. Res. 135 (2006) 394.
[24] W.R. Hewitt, E.M. Brown, G.L. Plaa, Toxicol. Lett. 16 (1983) 285.
[25] P.-J. Ferret, R. Hammoud, M. Tulliez, A. Tran, H. Trebeden, P. Jaffray, B. Malassagne, Y. Calmus, B. Weill, F. Batteux, Hepatology 33 (2001) 1173.
[26] X. Huang, Y.-F. Gong, K. Yu, Y.-Y. Cheng, Chinese J. Anal. Chem. 35 (2007) 1736.
[27] R.O. Recknagel, E.A. Glende, J.A. Dolak Jr., R.L. Waller, Pharmacol. Ther. 43 (1989) 139.
[28] K.K. Singh, Oxidative Stress, Disease and Cancer, Imperial College Press, London, 2006.
[29] A.F. Slater, Biochem. J. 222 (1984) 1.